STUK-YTO-TR 123
FEBRUARY 1997

Corrosion behaviour of zinc and aluminium in simulated nuclear accident environments

J. Piippo, T. Laitinen, P. Sirkiä
VTT Manufacturing Technology

In the Finnish Centre for Radiation and Nuclear Safety
the study was supervised by
Timo Karjunen

This study was conducted by order of
the Finnish Centre for Radiation and Nuclear Safety

FINNISH CENTRE FOR RADIATION AND NUCLEAR SAFETY
P.O.BOX 14, FIN-00881 HELSINKI, FINLAND
Tel. +358-9-759881
Fax +358-9-75988382

ISBN 951-712-177-6
ISSN 0785-9325

Oy Edita Ab
Helsinki 1997

PIIPPO, Juha, LAITINEN, Timo, SIRKIÄ, Pekka (VTT Manufacturing Technology). Corrosion behaviour of zinc and aluminium in simulated nuclear accident environments. STUK-YTO-TR 123. Helsinki 1997. 25 pp.+ Appendices 5 pp.

ISBN 951-712-177-6
ISSN 0785-9325

Keywords: zinc, aluminium, corrosion, hydrogen, accidents, particulates, sludge

ABSTRACT

Zinc and aluminium are used as anodic coatings and isolation materials in nuclear power plants. At high temperature environment they are supposed to oxidise and produce large amounts of hydrogen which is a danger for the power plant safety. The solid corrosion products may, together with insulation debris created as a result of a pipe break, also clog the pump suction strainers.

The solubility of zinc and aluminium and the stability of the corrosion products were estimated using thermodynamical calculations. The corrosion rates of zinc and aluminium were determined in simulated large pipe break and in simulated severe accident cases. An in situ on line measurement technique, which is based on the resistance measurement of sample wires, was used.

In the large pipe break case the corrosion rates of zinc and aluminium were determined at pH 8 and pH 10 in deaerated and in aerated solutions. Tests were also performed in aerated 0.1 M borate buffer solution at pH 9.2. Temperature range was 130°C...50°C. The corrosion of zinc appears to be relatively fast in neutral or mildly alkaline aerated water, while both high pH and deaeration tend to reduce the corrosion rates of zinc. The aeration and pH elevation decrease the corrosion rate of aluminium. Borate content increased especially the corrosion rate of aluminium.

The simulation of the severe accident case took place in the pH range 3–11 in chloride containing solutions at 50°C temperature. The corrosion rate of aluminium was lower than that of zinc, except for the solution with pH 11, in which the corrosion rate of aluminium was practically identical to that of zinc. Both metals corroded more rapidly in the presence of chlorides in acidic and alkalic conditions than in the absence of chlorides at neutral environment. The behaviour of zinc and aluminium was also monitored in high temperature water at 170°C and steam at 300°C.

The experimental results showed that the corrosion rate of zinc decreases with increasing pH, which is in agreement with the decreasing solubility of zinc with increasing pH observed in thermodynamical calculations. The solubility of zinc decreased as the temperature was increased. According to the calculations ZnO is the stable form of the corrosion products of zinc, which was in agreement with the experimental results.

PIIPPO, Juha, LAITINEN, Timo, SIRKIÄ, Pekka (VTT Valmistustekniikka). Sinkin ja alumiinin korroosio ydinvoimalaitosonnettomuutta simuloivissa olosuhteissa. STUK-YTO-TR 123. Helsinki 1997. 25 s.+ liitteet 5 s.

ISBN 951-712-177-6
ISSN 0785-9325

Avainsanat: sinkki, alumiini, korroosio, vety, onnettomuudet

TIIVISTELMÄ

Sinkkiä ja alumiinia käytetään pinnoite- ja eristemateriaaleina ydinvoimalaitoksissa. Mahdollisen onnettomuuden yhteydessä niiden oletetaan hapettuvan korkeassa lämpötilassa ja tuottavan suuria määriä vetyä, mikä voi vaarantaa ydinvoimalaitoksen turvallisuuden. Hapettumisen yhteydessä syntyvät kiinteät korroosiotuotteet sekä putken rikkoutumisen yhteydessä vapautuneet eristeriekaleet voivat myös tukkia kiertovesipumppujen imusiivilöitä.

Sinkin ja alumiin liukoisuutta ja niiden korroosiotuotteiden stabiilisuutta arvioitiin termodynaamisten laskelmien avulla. Sinkin ja alumiinin korroosionopeudet määritettiin ydinvoimalaitosonnettomuuksia simuloivissa ympäristöissä. Mittauksissa käytettiin in situ menetelmää, joka perustuu koekappaleina käytettyjen näytelankojen sähkövastuksen mittaukseen.

Ydinvoimalaitoksen höyryputkirikkoa kuvaavaa onnettomuutta simuloitiin hapettomissa ja hapellisissa liuoksissa pH arvoilla 8 ja 10. Lisäksi kokeita suoritettiin boraattipuskuriliuoksessa, jonka pH oli 9.2. Sinkin ja alumiinin korroosionopeudet määritettiin lämpötiloissa 130°C...50°C. Sinkin korroosio on suhteellisen nopeaa neutraaleissa ja lievästi emäksisissä ympäristöissä. pH:n nosto ja hapen poisto liuoksessa pienentivät sinkin korroosionopeutta. Hapen poisto liuoksesta ja pH:n nosto lisäsivät alumiinin korroosionopeutta. Alumiini liukeni nopeasti boraattipuskuriliuoksessa.

Vakavaa onnettomuutta simuloitiin pH arvoilla 3–11 50°C lämpötilassa siten, että happamissa ja emäksissä olosuhteissa liuos sisälsi klorideja. Alumiinin korroosionopeus oli pienempi kuin sinkin, paitsi pH:ssa 11, jossa niiden korroosionopeudet olivat samat. Molemmat metallit syöpyivät nopeammin klorideja sisältävissä olosuhteissa happamissa ja emäksisissä ympäristöissä kuin kloridittomassa neutraalissa ympäristössä. Sinkin ja alumiinin korroosionopeudet määritettiin myös 170°C lämpöisessä vedessä ja 300°C lämpöisessä höyryssä.

Tasapainolaskelmien mukaan pH:n nosto pienentää sinkin liukoisuutta, minkä myös kokeet vahvistivat. Laskennallisten arvioiden mukaan sinkin liukoisuus pienenee lämpötilan kohotessa. Kokeet ja termodynaamiset laskelmat osoittivat, että sinkkioksidi (ZnO) on stabiili kiinteä korroosiotuote.

CONTENTS

NOMENCLATURE

l = wire length
m = mass
r = wire radius
R = electrical resistance
t = time
ρ_r = specific resistance of a material
ρ_d = density of a material

1 INTRODUCTION

The containment buildings both in pressurised water reactors (PWR's) and boiling water reactors (BWR's) house large quantities of zinc and aluminium. Zinc can be found in zinc-based paints and galvanised surfaces in steel liners, cable trays, conduits, walkways, gratings, insulation covers, and various supports, while aluminium is used in fans, blades, hubs, and valves, for example. The zinc and aluminium masses present in the containment may vary greatly depending on the plant design, but values as high as 10–20 tons of zinc and 1–10 tons of aluminium have been given for certain plants.

During normal operation, when containment atmosphere is dry and the temperatures are moderate, corrosion of zinc and aluminium is very slow. However, in accident situations the conditions can be very different. For example, in the case of a large pipe break nearly all surfaces in the containment may be wetted with hot water. Provided that the surface area prone to corrosion is large, considerable quantities of both gaseous and solid corrosion products can be formed. The release of a gaseous product, namely hydrogen, may increase the containment pressure and cause fires. Slow pressurisation can be important especially in the inerted containments, where very little oxygen is available for recombination. The solid corrosion products in turn may affect both the functioning of the systems for cooling water recirculation and cleaning, and the behaviour of the fission products dissolved in the cooling water.

Corrosion of zinc and aluminium was studied quite intensively in the 1970's and the early 1980's [1–8] The studies were limited to the assessment of the hydrogen production potential in a case of a large pipe break, which formed the design basis for the reactor containments. Based on these studies, it has been concluded that in accidents which do not result in extensive fuel overheating, hydrogen is predominantly produced by corrosion of zinc-based paints, galvanised materials and aluminium, together with water radiolysis.

A major shortcoming in these studies is that little or no attention was paid to the formation of solid corrosion products. Consequently, they did not provide any data that could be used when assessing for example the pump suction strainer performance during a large pipe break. This issue was reopened after the Barsebäck incident in 1992, in which inadvertent relief valve blow down directly to the upper drywell of the containment damaged pipe insulation and caused clogging of the core and containment spray suction strainers. Since then a lot of attention has been paid to estimate the nature and amount of debris present in the containment water pools during an accident. While detailed analysis has been made concerning the corrosion products present in the pools during normal operation, no such assessment has been possible for the corrosion products produced during an accident.

Since also severe accidents involving considerable core damage have been brought under investigation, the data base concerning corrosion of zinc and aluminium has become insufficient even for the estimation of hydrogen production potential alone. During severe accidents the containment may be pressurised allowing water temperature to be higher than in the design basis accidents. If also the containment cooling is lost, the containment materials may contact superheated

steam flowing directly from the primary circuit. This high temperature range was not covered in the early experiments.

Corrosion during a severe accident may be enhanced also due to the release of chloride, which is contained in the cable insulation material during normal operation. Yet the effects of chloride on the corrosion of zinc and aluminium have not been studied.

This report describes a set of experiments that were performed in order to obtain quantitative data on corrosion rates and solid products of zinc and aluminium in conditions typical for both design basis and severe accident conditions. The experiments were performed by VTT Manufacturing Technology on the contract of the Finnish Centre for Radiation and Nuclear Safety (STUK).

2 EQUILIBRIUM SOLUBILITY OF ALUMINIUM AND ZINC

2.1 Background

Both soluble species and solid corrosion products can be formed when aluminium and zinc are oxidised in an aqueous environment. The nature of the corrosion products depends on the prevailing conditions. If the physical and chemical conditions (e.g. pH) vary in the vessel, release of soluble species to the aqueous environment at one location may lead to precipitation of solid products in the other parts of the vessel. The starting point for the understanding of the dissolution and precipitation behaviour of aluminium and zinc and their relevant oxidation products is based on thermodynamic equilibrium calculations.

Niyogi et al. [5] reviewed solubility product data for compounds assumed to control the solubility of aluminium and zinc in the temperature range 20...30 °C. They used the concept of aluminium hydroxides to refer to such compounds as $Al_2O_3 \cdot 3H_2O$ ($Al(OH)_3$) and $Al_2O_3 \cdot H_2O$ (AlO(OH)). Aluminium hydroxide precipitates were, under certain conditions, suggested to undergo a recrystallization process through intermediate hydration states to more stable and less soluble forms. For instance, aluminium hydroxide might in acidic conditions initially precipitate as $Al(OH)_3$, and then slowly convert to $Al_2O_3 \cdot 3H_2O$. On the other hand, in alkaline conditions aluminium hydroxide might initially precipitate as AlO(OH), and then convert to $Al_2O_3 \cdot H_2O$. The solubility data of Al presented in ref. [5] were based on the assumption that $Al(OH)_3$ and AlO(OH) determine the solubility of Al. Zinc was also assumed to precipitate as zinc hydroxide [5], the solubility product of which determines the concentration of total soluble Zn in the aqueous solution. In the presence of aqueous boron, precipitation of Zn as $Zn(BO_2) \cdot H_2O$ may also be of significance. Niyogi et al. [5] presented no results concerning solubility at higher temperatures.

Fineschi et al. [6] discussed the behaviour of aluminium in terms of different regions: at low pH values dissolution as Al^{3+}, at near neutral pH values passivation due to an aluminium oxide film, and at high pH dissolution as AlO_2^-. The oxide was reported to consist of $Al_2O_3 \cdot H_2O$ at room temperature and of $Al_2O_3 \cdot 3H_2O$ at temperatures above 75 °C.

It is worth noting that the thermodynamic properties of surface oxides may differ from those of bulk oxides (as commented also by Fineschi et al. [6]). The thermodynamic data available for solid oxidation products have most often been determined for bulk oxides, which results in some uncertainty in any equilibrium calculations for surface films. Also, it has to be taken into account that the surface films can only seldom be considered to be in an equilibrium state.

2.2 Thermodynamical calculations

In this work the equilibrium solubility of aluminium and zinc was estimated in different pH values and at different temperatures using Chemsage 3.0.1 software (GTT Technologies, Germany). The thermodynamic data for solid compounds were obtained from the HSC database (Outokumpu Research Oy, Finland) and for the aqueous species from GEM Aqua database (GEM Systems, Finland.).

The total concentration of dissolved Zn (present as $Zn^{2+}(aq)$, $HZnO_2^-(aq)$ and $Zn(OH)_2(aq)$) resulting in the precipitation of ZnO or $Zn(OH)_2$ in

three different conditions (25 °C and 3.5 bar, 80 °C and 3.5 bar, 165 °C and 7 bar) in the pH range 5–11 are given in Figure 1. ZnO limits the solubility of zinc in the whole pH range. The solubility of zinc decreases with increasing pH and with increasing temperature. The behaviour at 25 °C in Figure 1 is closely similar to the curve presented by Niyogi et al. [5].

The total concentration of dissolved Al (present as $Al^{3+}(aq)$, $AlO_2^-(aq)$ and $Al(OH)_4^-(aq)$) resulting in the precipitation of Al_2O_3 or $Al(OH)_3$ in three different conditions (25 °C and 3.5 bar, 80 °C and 3.5 bar, 165 °C and 7 bar) in the pH range 5–11 are given in Figure 2. Al_2O_3 limits the solubility of aluminium in the whole pH range. At room temperature the solubility of aluminium shows a minimum at pH 5.8, while at 80 °C and at 165 °C the solubility increases with pH over the whole pH range 5–11. The solubility increases with temperature (except for pH < 5). The curve for 25 °C in Figure 1 is qualitatively similar to the curve presented by Niyogi et al. [5].

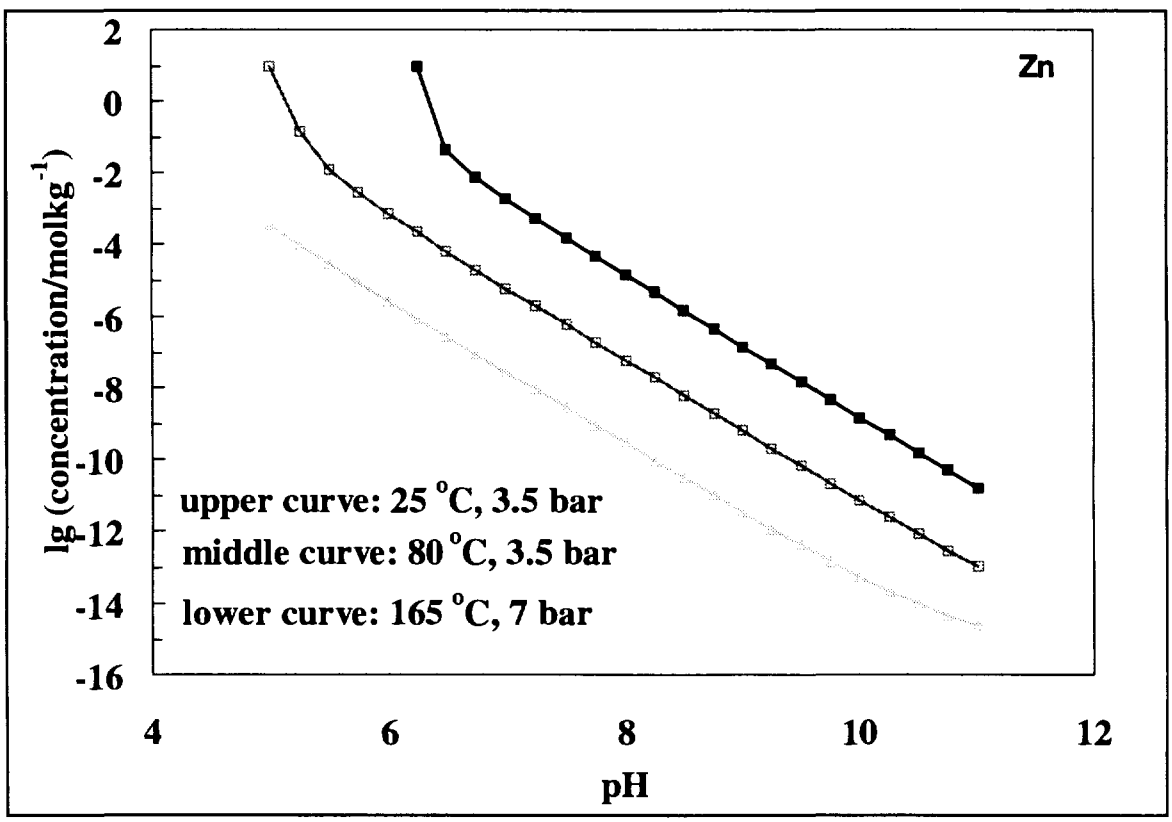

Figure 1. *The total solubility of zinc (as $Zn^{2+}(aq)$, $HZnO_2^-(aq)$ and $Zn(OH)_2(aq)$) in aqueous solutions in different conditions.*

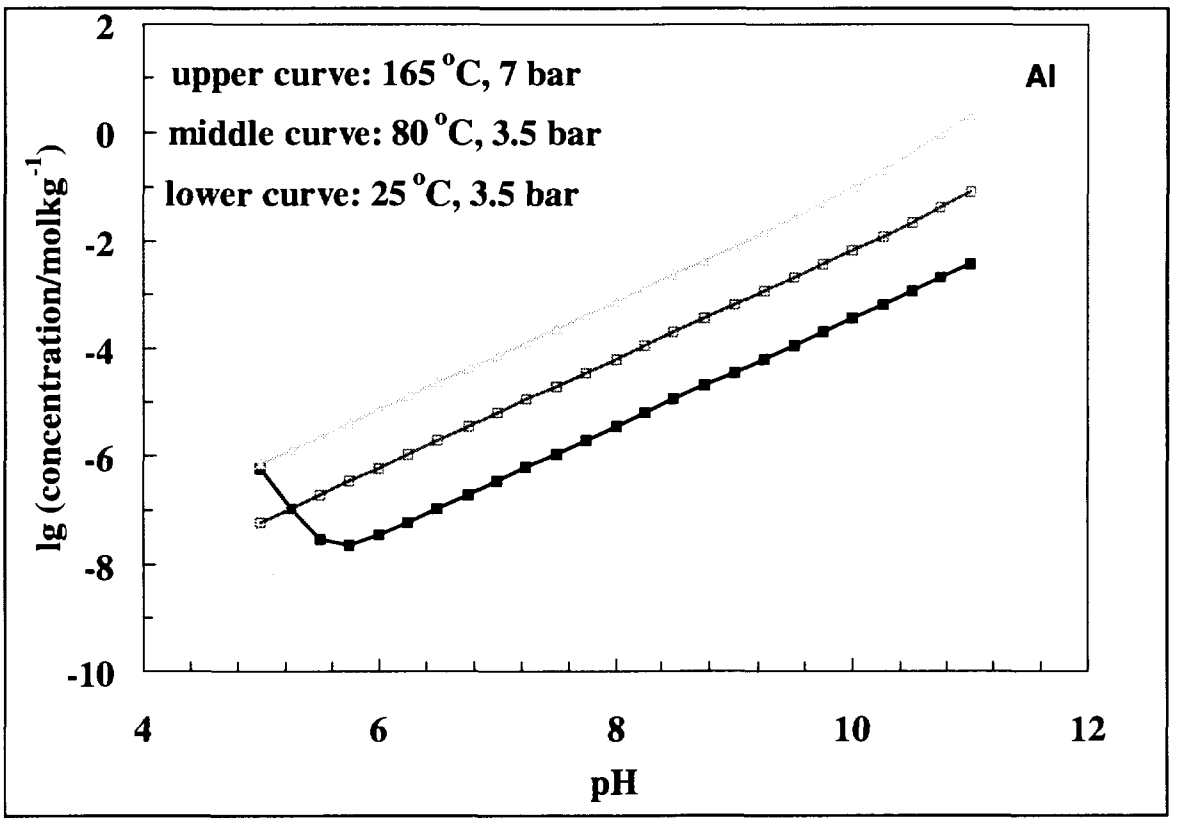

Figure 2. *The total solubility of aluminium (as $Al^{3+}(aq)$, $AlO_2^-(aq)$ and $Al(OH)_4^-(aq)$) in aqueous solutions in different conditions.*

3 TEST MATERIALS, EQUIPMENT AND EXPERIMENTAL PROCEDURES

Zinc and aluminium wires, aluminium plates and hot-dip galvanised steel plates were used as test materials. The chemical composition of the zinc and aluminium wires supplied by Goodfellow Ltd is presented in Table I. The aluminium plates and the hot-dip galvanised steel plates were taken from TVO NPP pipe installations and foot gratings, respectively.

Tests were performed in a titanium cladded autoclave equipped with necessary input and output pipelines and a temperature control. Temperatures varied from 300 °C to 50 °C depending on the test. Volume of the autoclave was 7 dm^3.

Water purified in a Milli-RO 15 water system (Millipore) was used as test solution. Its pH and chloride concentration was adjusted using lithium hydroxide (LiOH) and hydrochloric acid (HCl). In one test the pH of the solution was adjusted using 0.1 M $Na_2B_4O_7$ solution. All the chemicals were of pro analysis grade. The solutions were pumped from a reservoir via a filter into the autoclave and further cooled in a heat exchanger before returning to the reservoir. The volume flow of the solution was regulated to 10 ml/min by a pump in all the tests. The total volume of the solution was 20 dm^3 in each test.

The environment inside the autoclave was possible to adjust oxidising or non-oxidising by bubbling air or nitrogen through the solution, respectively. Both gases were decompressed to the desired pressure before supplying into the autoclave. The exact conditions of individual tests are described in the next chapter.

The diameter of the zinc and aluminium wires was 1 mm. The wires were coiled around Teflon bars in order to eliminate the short circuiting and

Table I. Chemical compositions of zinc and aluminium wires. All impurity contents are shown in ppm.

	Zinc	Aluminium
Item number:	ZN005150/1	AL007905/2
Cadmium:	7	
Calcium:		<1
Chromium:		<1
Copper:	<1	10
Iron:	<1	10
Lead:	20	
Magnesium:		2
Manganese:	<1	2
Silicon:	<1	15
Silver:	1	<1

in order to make a proper attachment possible when installed into an autoclave. The lengths of the wires varied from 12 m to 2 m depending on the test. The installation of the wires and of the aluminium plate are shown in Figure 3. The surface area of the aluminium plates was approximately 50 cm^2 and that of the steel plates approximately 6000 cm^2 which means that 120 fold area of zinc compared to that of aluminium was exposed to the test environment.

After the installation of the samples, the autoclave was pressurised, heated and the water circulation was started. After the test, the autoclave was opened and the samples were visually inspected. All the test materials were weighed before and after the tests (with and without oxide layer) in order to determine the weight loss rate. The loose oxides were removed from samples by washing them in 6 % NH_4OH -solution before weighing. Galvanised steel plates were weighed without cleaning.

A solution sample was taken from autoclave for pH measurement and for cation concentration analysis, if necessary. Cation concentration analysis was performed using atom absorption spectrometry (AAS). Oxidation products from the autoclave bottom were collected for chemical analysis and grain size characterisation. The chemical analysis of the corrosion products was performed using X-ray diffraction (XRD) and X-ray fluorescence (XRF) analysis.

The corrosion rates of zinc and aluminium wires were determined also by measuring on-line the electrical resistance of the corroding wires during the tests. Corrosion reduces the diameter of the metallic part of a wire as a function of time, which increases its electrical resistance. The measurement was performed by feeding a constant current of 100 mA through the wires using a Yokokawa 7651 power source. The voltage drop over the wire was measured using a Keithley 182 sensitive digital voltmeter at intervals of five or ten minutes. The data from the digital voltmeter was saved to a microcomputer. The electrical resistance was calculated from the voltage drop and the current using the Ohm's law.

Knowing the electrical resistance (R), its time derivative (dR/dt), the specific resistance of a material (ρ_r) and the wire length (l), it is possible to determine the wire radius decrease rate dr/dt as a function of time

$$\frac{dr}{dt}\left[\mu m/h\right] = -600000 \cdot 1/2 \cdot \sqrt{\frac{\rho_r \cdot l}{\pi}} \cdot R(t)^{-3/2} \cdot dR/dt \qquad (1)$$

The radius change rate is converted to weight loss rate because it is more informative. Conversion was performed by multiplying corrosion rate by the density of the material

$$\frac{dm}{dt}\left[g/m^2\ h\right] = \frac{dr}{dt} \cdot \rho_d \cdot 10^{-6} \cdot 10^3 \qquad (2)$$

where ρ_d is the density of material. Note that the tests were not reproduced. Thus no statistical estimation of the measurement accuracy could be made.

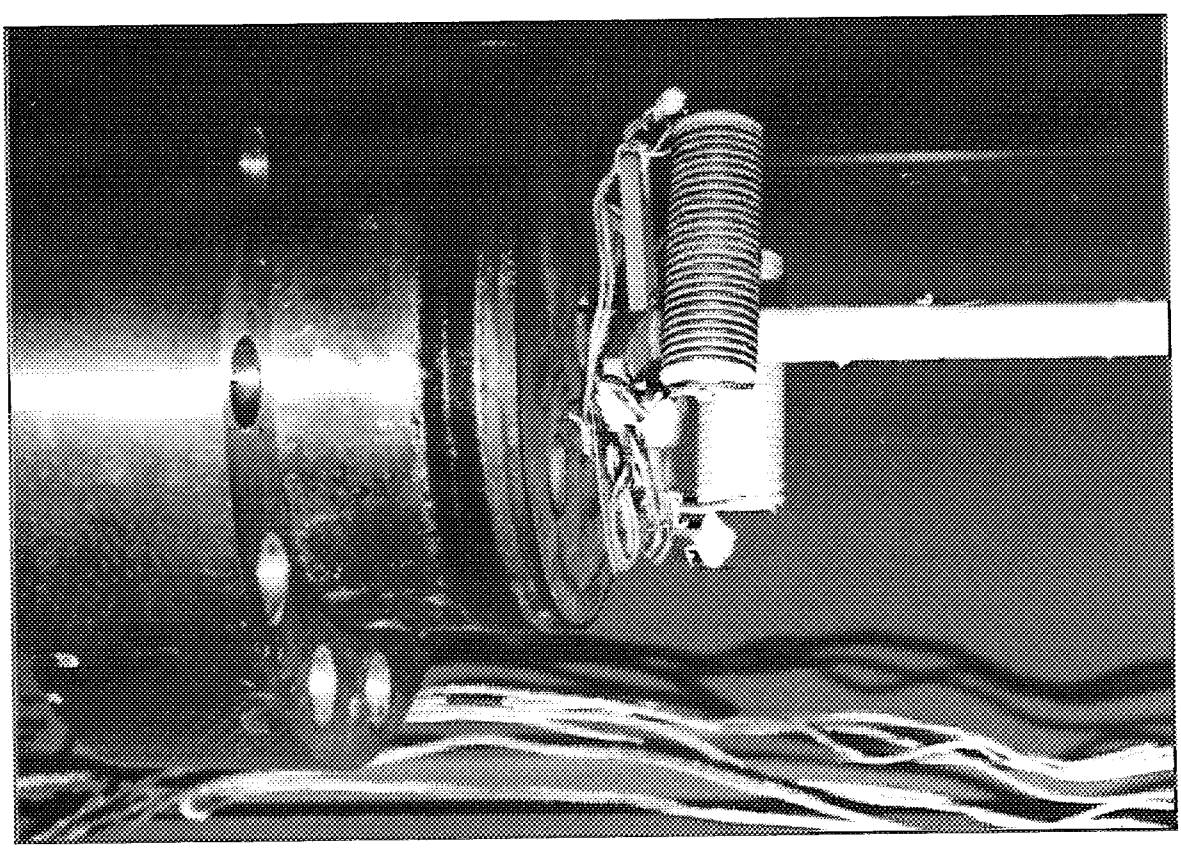

Figure 3. *Installation of wires and aluminium plate.*

The proportion of the oxide remaining on the wire surfaces was estimated by calculating the mass of the corroded metal using the corrosion rate data based on the resistance measurement method. All the zinc and aluminium was supposed to convert to ZnO and Al_2O_3, respectively. The hypothetical weight gain due to the oxide growth was calculated. The difference of the real weight gain and the calculated weight gain was compared to the mass of the oxide.

4 TEST CONDITIONS AND RESULTS

The performed tests can be divided into two groups according to the type of the accident they simulate. The first group (denoted with A) describes the material behaviour during a large pipe breakage accident (LOCA) and the second group (denoted with B) during a severe accident.

4.1 Large pipe break case

As a large steam or water pipe breaks during a LOCA accident in a reactor containment, temperature and pressure are controlled using containment spray systems. At the beginning of the accident the temperature is high but it decreases rapidly.

A summary of the test conditions is given in Table II. At the beginning of tests the temperature was 130°C, and it was lowered stepwise to 50°C. The testing periods took approximately one day at 130°C and at 110°C, and two days at the other temperatures. pH values 8 and 10 were used in order to simulate the effect of LiOH that is added into spray water in BWR's for the iodine chemistry control. The effect of redox potential on the corrosion rates was studied by performing the tests in oxygen-free water and in water saturated with air. Borate buffer solution (pH 9.2) was used in one test in order to simulate the accident taking place in a VVER-440 environment.

Table II. Test conditions in large pipe break experiments.

Test Nr.	T / °C	pH/beginning	pH/end	Environment	Time	Note
A1	130 110 90 70 50	8	6.5	H_2O + LiOH	6 h 36 h 2 d 2 d 2 d	N_2-pressurisation 500 dm^3/h
A2	130 110 90 70 50	8	7.1	H_2O + LiOH	1 d 1 d 3 d 2 d 2 d	air-pressurisation 500 dm^3/h
A3	130 110 90 70 50	10	9.4	H_2O + LiOH	1 d 1 d 2 d 2 d 3 d	N_2-pressurisation
A4	130 110 90 70 50 70 90 110 130	10	9.4	H_2O + LiOH	1 d 1 d 2 d 2 d 2 d 1 d 1 d 1 d 1 d	air-pressurisation 500 dm^3/h
A5	130 110 90 70 50	9.2	9.3	H_2O + $Na_2B_4O_7$	1 d 1 d 2 d 2 d 2 d	air-pressurisation

Table III. The concentrations of dissolved Zn, Fe and Al in the process solutions after the tests.

Test Nr.	Environment	Gas	Cation concentration		
			Zn / mg/l	Fe / µg/l	Al / µg/l
A1	pH 8	N_2	21.5	30	—
A2		air	3.4	6	< 10
A3	pH 10	N_2	2.7	5	< 10
A4		air	1.8	6	< 10
A5	borate, pH 9	air	64.5	690	18 500

4.1.1 Analysis of corrosion products

The average grain size of all the corrosion products from the autoclave bottom was 10 µm. The results for individual tests are given in Appendix 1.

When considering the results of the chemical analyses of corrosion products, it has to be taken into account that the surface area of the corroding aluminium plate was much smaller than that of the galvanised steel plates. X-ray fluorescence analysis indicated that the solid deposits formed as a result of corrosion consist in all tests mainly of Zn and O. ZnO was found to be the main compound on the basis of X-ray diffraction analysis, although the presence of amorphous $Zn(OH)_2$ cannot be excluded either.

The concentrations of dissolved zinc, iron and aluminium in the test solutions determined using AAS are presented in Table III.

The concentration of dissolved zinc decreases with increasing pH in water containing no borate. The Al content was in these cases below the detection limit. The addition of borate increased strongly the solubility of Zn, Al and Fe.

4.1.2 Corrosion of zinc

Figure 4 shows the corrosion rate of zinc based on the measurement of the electric resistance, while the numerical values are given in a table in Appendix 2.

The proportion of the oxide remaining on the zinc wire surface, the results based on the measurement of the weight loss of zinc wires and galvanised steel plates together with a description of the oxidation product on the wires and the plates are given in Table IV. The calculations show that major part of the zinc oxide remains on the wire surface.

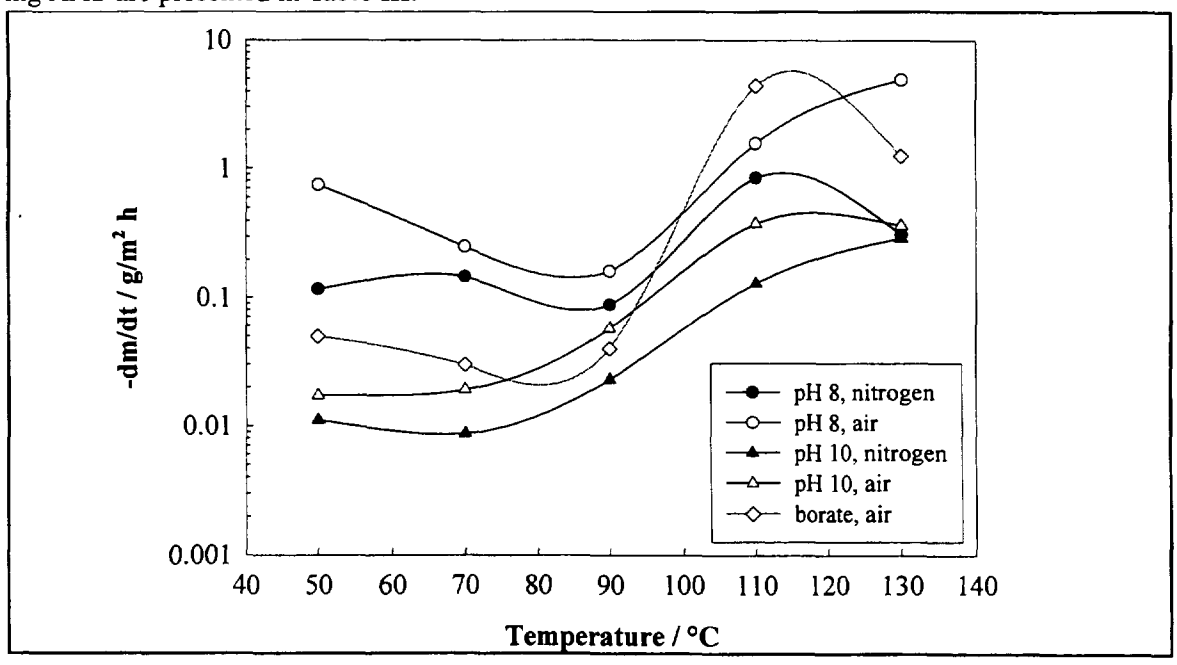

Figure 4. Corrosion rates (converted to g/m²h) for zinc as a function of temperature in different pH and gas environments determined by measuring the resistance increase of the corroding wires.

Table IV. *Description of the corrosion products of zinc formed on zinc wires and on galvanised steel plates together with the weight loss data of the wires and plates in the large pipe break experiments.*

	Run A1		Run A2		Run A3		Run A4		Run A5	
	Zinc wire	**galvanised steel plates**	**Zinc wire**	**galvanised steel plates**	**Zinc wire**	**galvanised steel plates**	**Zinc wire**	**galvanised steel plates**	**Zinc wire**	**galvanised steel plates**
Visual inspection	Dark coloured oxide layer on the wire.	Slight corrosion visible on the samples.	Light brown coloured powdery oxide layer on the wire.	Plentiful of powdery corrosion products on the samples. Coloured light brown	Wire covered by dark coloured oxide layer	Some powdery corrosion products visible on the samples.	Powdery oxide layer on the wire, not formed regularly	Powdery corrosion products on the samples. Coloured light brown	Wire covered by dark oxide layer	Oxide layer not visible. Some dark spots. Surface coarse.
Change of weight (with oxide layer) [%]	0.14	0.09	–0.18		–0.02		–0.26		0.88	
Change of weight (Washed) [%]	–0.06		–3.26	0.24	–0.04	0.13	–0.37	0.18	0.43	0.11
Change of weight (without oxide layer) [%]			–4.60		–0.43		–1.08		–1.28	
Proportion of ZnO remaining on surface [%]	90		80		80		70		90	

4.1.3 Corrosion of aluminium

Figure 5 shows the corrosion rate of aluminium based on the measurement of the electric resistance, while the numerical values are given in Appendix 2.

The proportion of the oxide remaining on the aluminium wire surface, the results based on the measurement of the weight loss of aluminium plates together with a description of the oxidation products on aluminium wires are given in Table V. At pH 8 and 10 major part of the oxide remains on the surface. The pH elevation increases the proportion of oxides remaining on surface by about 20 %-units. In the borate containing solution only about 20 % of the oxide stays on the aluminium surface.

4.2 Severe accident case

If the spraying systems do not work during a LOCA the temperature in the containment remains high for a long time. The high temperature affects the corrosion rates of structural materials in the containment and it can also increase the decomposition rate of the cable insulation materials. The decomposition may cause the release of gases containing chloride that affects the corrosion of structural materials in the containment.

A summary of the test conditions is given in Table VI. Experiments were performed using zinc and aluminium wires as test materials.

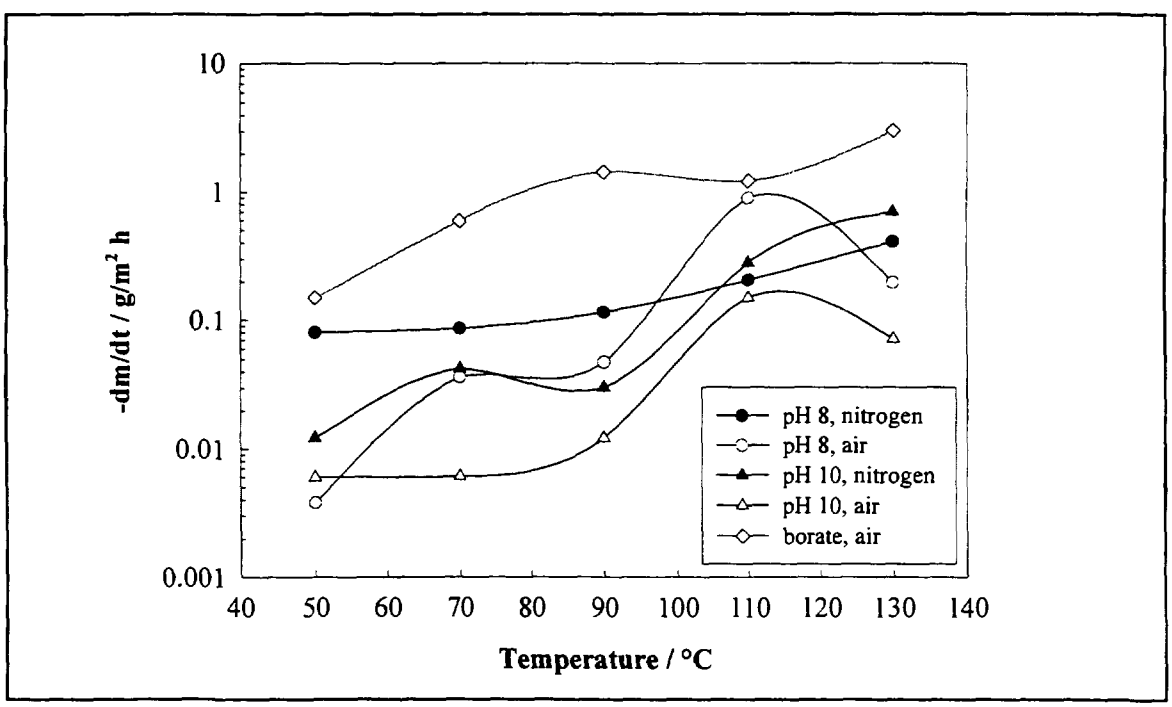

Figure 5. *Corrosion rates (converted to g/m²h) for aluminium as a function of temperature in different pH and gas environments determined by measuring the resistance increase of the corroding wires.*

Table V. *Description of the corrosion products of aluminium wires and plates together with the weight loss data of the wires and plates in the large pipe break experiments.*

	Run A1		Run A3		Run A5					
	Aluminium wire	**Aluminium plate**	**Aluminium wire**	**Aluminium plate**	**Aluminium wire**	**Aluminium plate**	**Aluminium wire**	**Aluminium plate**	**Aluminium wire**	**Aluminium plate**
Visual inspection	Wire covered by thin oxide layer.	Plate covered by thin oxide layer.	Wire covered by thin oxide layer.	Plate covered by thin oxide layer.	Very thin oxide layer on the wire	Brightness faded, thin oxide layer	Very thin oxide layer on the wire	Light oxide layer with white corrosion spots on lower side, upper side darkened	Light oxide layer of the wire. Surface was corroded	Surface was corroded
Change of weight (with oxide layer) [%]	0.59	0.50	0.98	1.69	2.22	0.45	1.63	0.66	−11.51	−10.71
Change of weight (washed) [%]	0.10	0.28	0.73	1.34	2.18	0.43	1.57	0.43	−13.31	−12.19
Change of weight (without oxide layer) [%]			0.60	0.34	2.11	0.41	1.53	0.38	−14.67	−13.38
Proportion of Al2O3 remaining on surface [%]	60		60		80		80		20	

Table VI. Test conditions in experiments where a severe accident was simulated. The pH values are measured at the beginning of experiments.

Test Nr.	T / °C	pH	Environment	Time	Observe
Run B1	300	—	Superheated steam	1d	
Run B2	170	~6.5	H_2O + $[O_2]$~200 ppb	4 d	water flow 0.2 dm^3/min
Run B3	50	~7	H_2O + $[O_2]$~8 ppm at start	4 d	
Run B4	50	5.07	H_2O + 1E–5 mol/l HCl	4 d	N_2-overpressure
Run B5	50	3.0	H_2O + 1E–3 mol/l HCl	3 d	N_2-overpressure
Run B6	50	9. 0	H_2O + 5E–4 mol/l HCl + 5.6E–4 mol/l LiOH	5 d	N_2-overpressure
Run B7	50	11.0	H_2O + 5E–4 mol/l HCl + 7E–3 mol/l LiOH	5 d	N_2-overpressure

4.2.1 High temperature tests

These measurements simulated the early time sequence in an accident as the hot steam (300 °C) is discharging from a broken cooling water pipe (Run B1) and the later period as the water has cooled to 170°C (Run B2).

Pure water deaerated with nitrogen was used as test solution. The water was pumped on to the autoclave bottom where it was evaporated and superheated at the test temperature of 300 °C. In the experiments performed at 170°C the dissolved oxygen content of the input water was controlled to be 200 ppm ± 20 ppm. The results are summarised in Table VII.

The average grain size of the oxide product deposit formed at 170 °C was ca. 30 μm.

4.2.2 Effect of chloride

The effects of chloride concentration and pH were studied by making tests at uniform temperature of 50 °C. The pH was varied from 3 to 11 and the chloride concentration was varied from 1E–5 mol/l to 1E–3 mol/l. The results based on the measurement of the resistance of the zinc and aluminium wires are presented in Figure 6, while the corresponding numerical values are given in Appendix 3.

Table VII. Description of the corrosion products together with the weight loss data for zinc and aluminium in the severe accident experiments.

	Run B1 (300 °C)		Run B2 (170 °C)		
	Zinc wire	Aluminium wire	Zinc wire	Aluminium wire	Galvanised iron wire
Visual inspection	The lowest part covered by a strong oxide. Rest of wire covered by light oxide layer.	No visual changes observed.	Abundant corrosion products in autoclave. Wire brittle, covered with black deposit. Wire extended approximately 5 m.	Thick loose layer of oxide. Wire extended approximately 1 m.	General corrosion, grey coloured.
Change of weight [%]	0.099	–0.001	–51.35	–47.50	
Weight loss rate [g/(m^2h)]	3.00	0.05	11.27	7.15	

Table VIII. The relative weight loss data of zinc and aluminium wires.

Run Nr.	pH	[HCl] / mol/l	[LiOH] / mol/l	Zn / $m-m_0/m_0$ / %	Al / $m-m_0/m_0$ / %
B5	3	$1.0 \cdot 10^{-3}$	—	–0.37	0.57
B4	5	$1.0 \cdot 10^{-5}$	—	–0.18	0.84
B3	7	—	—	–0.13	0.93
B6	9	$5.0 \cdot 10^{-4}$	$5.6 \cdot 10^{-4}$	–0.33	1.84
B7	11	$5.0 \cdot 10^{-4}$	$7.0 \cdot 10^{-3}$	–0.23	0.35

The corrosion rate of aluminium is lower than that of zinc, except for the solution with pH 11, in which the corrosion rate of aluminium is practically identical to that of zinc. Both metals seem to corrode more rapidly in the presence of chlorides in neutral and acidic conditions than in the absence of chlorides at neutral pH.

During the tests the dimensions of the wires did not change. At pH 3 zinc was covered by a dark oxide layer and the aluminium by a thin light coloured layer. At pH 5 both the materials had thin oxide layers. In neutral solution zinc had a light coloured brittle oxide layer and aluminium a very thin oxide layer. At pH 9 the zinc wire was covered by a light powdery layer. Corrosion products were observed on the bottom of the autoclave. No signs of oxide formation could be detected on aluminium. At pH 11 aluminium was covered by a thin oxide layer whereas no changes on the zinc wire surface could be observed.

The results of the relative corrosion rate determination based on weight loss measurements of zinc and aluminium wires are presented in Table VIII. Results show that the corrosion rate of aluminium wires could not be determined by means of the weight loss method because their weight increased due to the oxide formation in all the tests

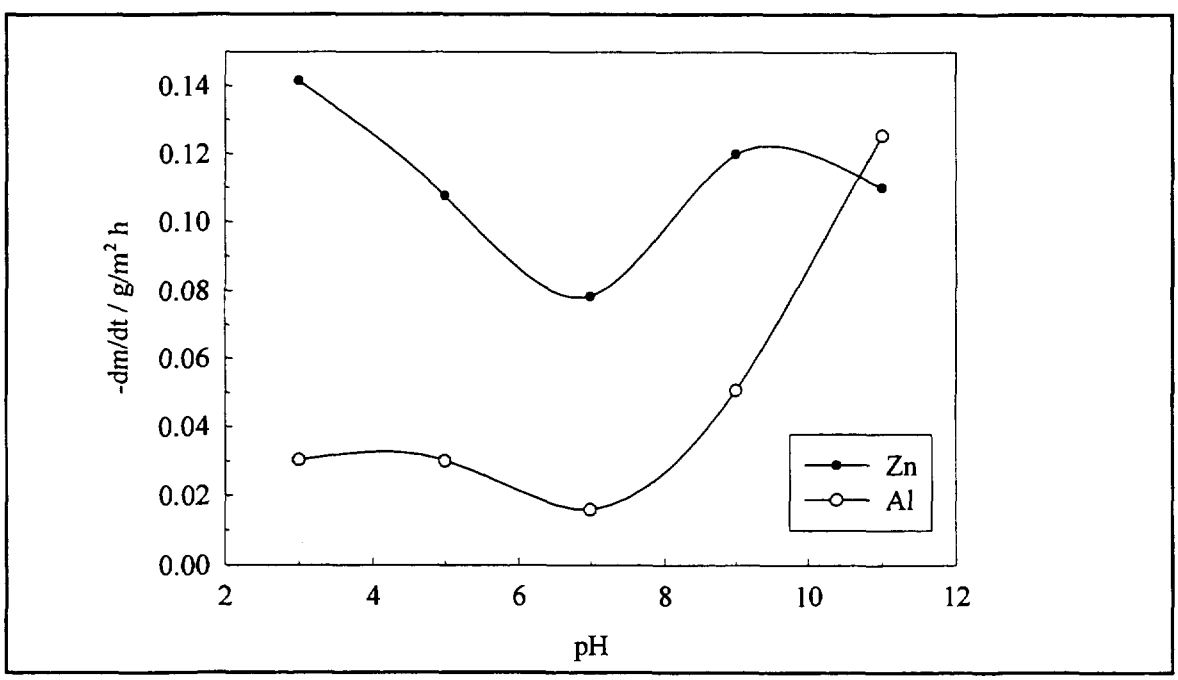

Figure 6. *The corrosion rates (converted to g/m² h) of zinc (closed symbols) and aluminium (open symbols) based on the measurement of the resistance of the wires in different environments. The compositions of the test solutions are presented in Table VI.*

5 DISCUSSION

5.1 Experimental observations

The corrosion rates were determined using weighing and a technique based on the measurement of electric resistance of wires. The resistance measurement was found to be more suitable in this study because it is an in situ technique and because the corrosion products on the specimens did not affect the results.

5.1.1 Large piper break case

The measurements show that the corrosion rates of zinc and aluminium may vary greatly depending on the water temperature and chemistry. Corrosion of zinc appears to be relatively fast in neutral or mildly alkaline aerated water, while high pH and deaeration both tend to reduce the corrosion rates. The use of borated alkaline water induces rapid corrosion at high temperatures, while at temperature range 50°C...90°C corrosion rates are moderate. Contrary to expectations, zinc corrosion did not always slow down when temperature decreased. In some cases a change in pH during the tests may have contributed to this unexpected behaviour. However, the same was evidenced also in the test with borated water, in which pH remained stable. This behaviour must be connected with the decreasing solubility of ZnO with decreasing temperature.

A lot of data on aluminium and zinc corrosion is available but only few of these are similar to the environments of this test series. The results obtained for zinc in borate containing solution can be compared to the data presented in [2, 3] shown in Figure 7. The measurements were performed in aerated 0.1 M borate solution at pH 9 [2] and in solutions containing 2000 ppm and 4000 ppm B at pH 9 [3]. Estimates by the same authors are also presented.

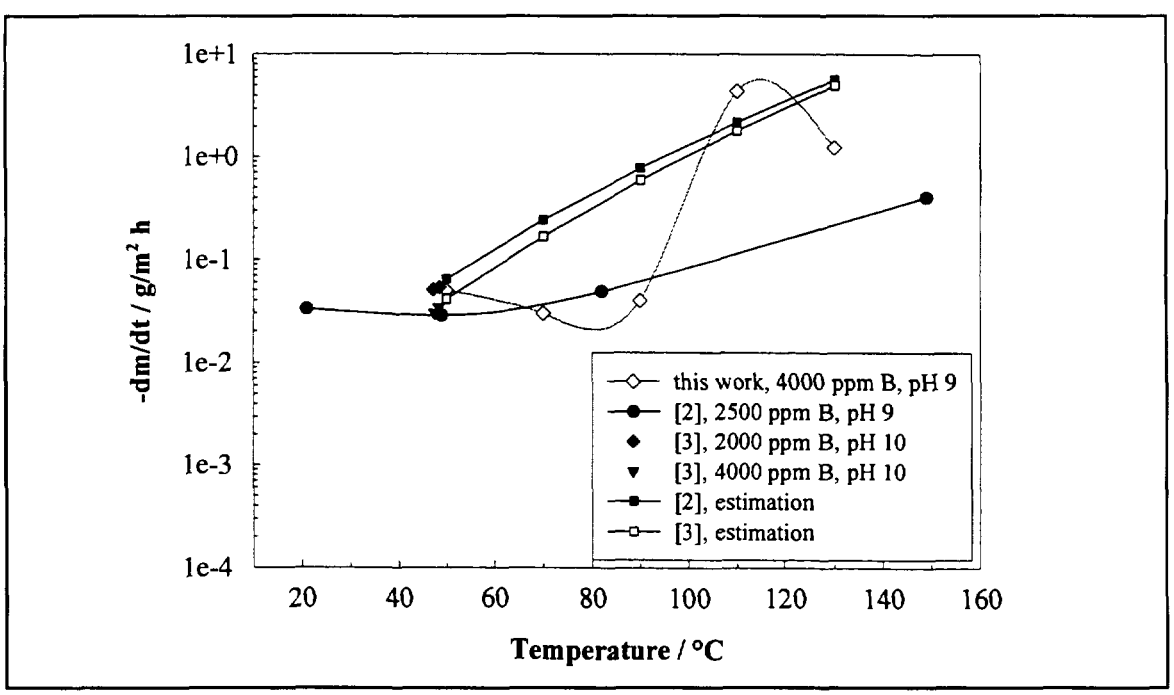

Figure 7. A comparison of estimated corrosion rate data [2, 3] for zinc and of zinc measured in 0.1 M borate buffer solution at pH 9 and of galvanised steel measured by [2, 3].

The corrosion rates are in good accordance at temperatures below 100°C, but at higher temperatures the corrosion rates obtained in this work are higher. The estimated corrosion rates [2] are somewhat higher at temperature region from 70°C to 90°C than the experimentally obtained corrosion rates in this work.

5.1.2 Severe accident case

Both zinc and aluminium are more susceptible to corrosion in the presence of chlorides in neutral and acidic conditions than in the absence of chlorides at neutral pH. The corrosion rate of aluminium is lower than that of zinc, except for the solution with pH 11, in which the corrosion rate of aluminium is practically identical to that of zinc.

Loyola and Womelsduff [3] have measured the hydrogen formation rate on galvanised steel in demineralised water at 48°C temperature. They observed a corrosion rate of 0.088 g/m^{2}h that is in good accordance to 0.079 g/m^{2}h measured for zinc in this study at pH 5 in the presence of chlorides. On the other hand, their result 39.4 g/m^{2}h at the temperature of 168°C is clearly higher than 11.3 g/m^{2}h measured for zinc at 170°C in this study.

Frid et al. had determined the corrosion rates of technically pure aluminium (AA 1050) in deaerated water at pH 5 at temperatures 50°C, 100°C and 150°C [4]. The corrosion rate was independent of temperature and exposure time. The corrosion rate of 14.4 mg/m^{2}h is lower than the 30 mg/m^{2}h observed in this study. Same authors repeated the same tests at pH 9 and obtained a corrosion rate of 12.6 mg/m^{2}h. As presented in Figure 7 and in Appendix 3 a somewhat higher corrosion rate of 51 mg/m^{2}h was obtained in this study. The higher corrosion rates obtained in this study are probably due to the chlorides.

5.2 Experimental results vs. thermodynamical calculations

The results of the analysis of the corrosion products, and the experimentally observed corrosion behaviour of zinc and aluminium agree in several aspects with the results of the thermodynamic calculations.

Equilibrium calculations indicated that the solid corrosion product should be in the form of ZnO, which was also detected in XRD analysis. On the other hand, the concentration of dissolved zinc decreases with pH in water containing no borate, which also agrees with the theoretical calculations reported in Chapter 1. Unfortunately, the content of dissolved aluminium and the amount of solid corrosion products of aluminium were too low to be detected with the methods used. Accordingly, no comparison between the theoretical calculations and the experimental results could be made.

The corrosion rate of zinc (determined by means of the measurement of the electric resistance of a zinc wire) decreased with increasing pH, which is in agreement with the decreasing solubility of zinc with increasing pH. On the other hand, the experimental dependence of the corrosion rate of aluminium on pH was not so straightforward. The main trend seemed to be that aluminium corrodes more rapidly at a lower pH, which is not in agreement with the solubility calculations of aluminium. Therefore, it can be suggested that the corrosion of aluminium proceeds as a solid state process in which the role of solubility is not very significant.

6 CONCLUSIONS

The corrosion rates of zinc and aluminium were determined in simulated large pipe break and in severe accident cases. An in situ on line measurement technique that was based on the resistance measurement of the sample wire was used. The technique was well applicable to this work because of its in situ measurement possibility and of its high accuracy compared to the conventional weight loss measurement method.

In the large pipe break case the corrosion rates of zinc and aluminium were studied at pH 8 and pH 10 in deaerated and in aerated solutions and in 0.1 M borate buffer solution at temperatures 130°C...50°C. The corrosion of zinc appears to be relatively fast in neutral or mildly alkaline aerated water, while high pH and deaeration both tend to reduce the corrosion rates. The aeration and pH elevation decrease the corrosion rate of aluminium.

The simulation of the severe accident case took place in the pH range from 3 to 11 in chloride containing solutions. The corrosion rate of aluminium was lower than that of zinc, except for the solution with pH 11, in which the corrosion rate of aluminium was practically identical to that of zinc. Both metals corroded more rapidly in the presence of chlorides in acidic and alkalic conditions than in the absence of chlorides at neutral environment.

The solubility of zinc and aluminium and the stability of the corrosion products were estimated using thermodynamical calculations. The experimental results and the thermodynamical calculations were in fair agreement.

REFERENCES

[1] Griess JC, Bacarella AL. The corrosion of materials in reactor containment spray solutions. Nuclear Technology 10, 1971: 546–53.

[2] van Rooyen D. Hydrogen release rates from corrosion of zinc and aluminium. BNL-NUREG-24532 Informal report. May 1973: 1–37.

[3] Loyola VM, Womelsduff JE. The relative importance of temperature, pH and boric acid concentration on rates of H_2 production from galvanised steel corrosion. NUREG/CR 2812. November, 1983.

[4] Frid W, Karlberg G, Sundwall SB. Hydrogen generation from aluminium corrosion in reactor containment spray solutions. Proceedings of the Second International Conference on the Impact of Hydrogen on Water Reactor Safety. Albuquerque, New Mexico, October 3-7, 1982. NUREG/CP-0038. pp. 440–50.

[5] Niyogi KK, Lunt RR, Mackenzie JS. Corrosion of aluminium and zinc in containment following a LOCA and potential for precipitation of corrosion products in the sump. Proceedings of the Second International Conference on the Impact of Hydrogen on Water Reactor Safety. Albuquerque, New Mexico, October 3–7, 1982. NUREG/CP-0038. pp. 401–423.

[6] Fineschi F, Lanza S and Lombardi G. Hydrogen generation in LOCA conditions: the contribution of aluminium corrosion. Contribution to the Hydrogen Sub-Group, Working Group 2, Comitato Nazionale Energia Nucleare (Contract AC-3), EEC Bruxelles, December 1980: 1–58.

[7] Zittel HE. Post-accident hydrogen generation from protective coatings in power generations. Nuclear technology 19, 1973: 143–6.

[8] Lopata JR. Control of containment H_2 levels evolved from zinc primers during a LOCA. Power Engineering / November 1974: 48–51.

APPENDIX 1

The grain size distributions of the individual tests of the large pipe break case.

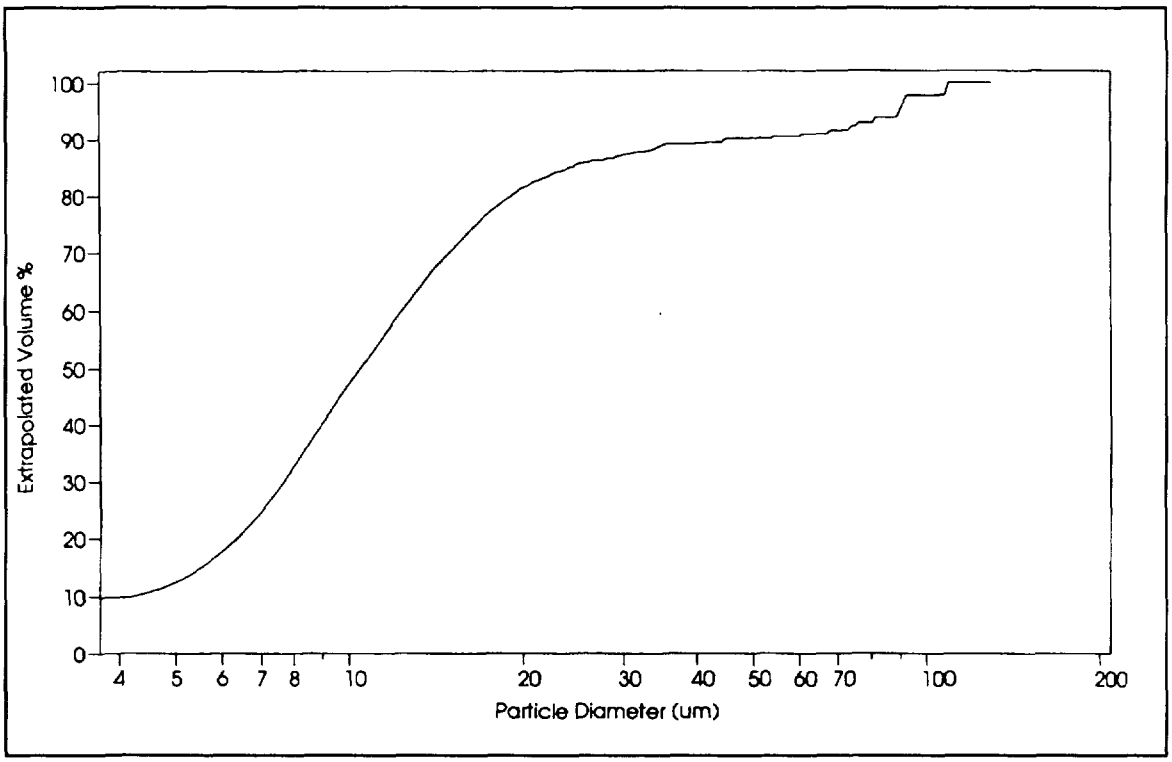

Figure A1-1. *The cumulative particle size distribution of the corrosion products obtained in test A1.*

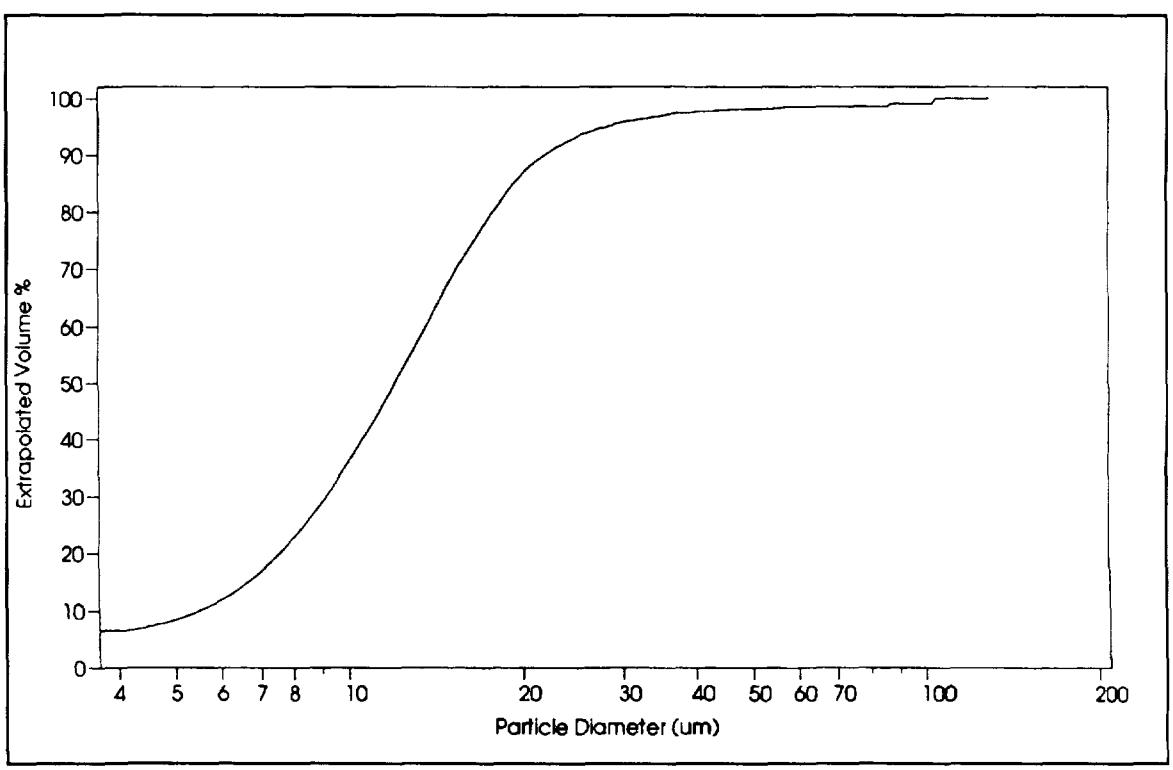

Figure A1-2. *The cumulative particle size distribution of the corrosion products obtained in test A2.*

APPENDIX 1

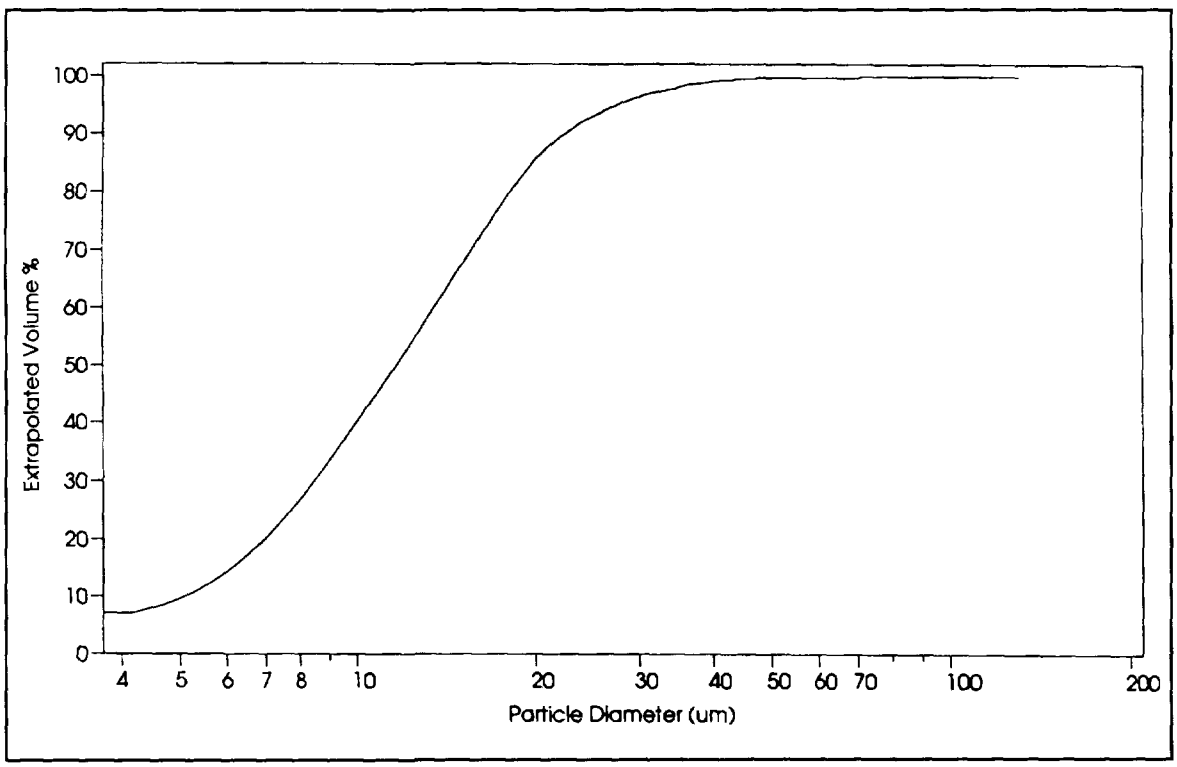

Figure A1-3. *The cumulative particle size distribution of the corrosion products obtained in test A3.*

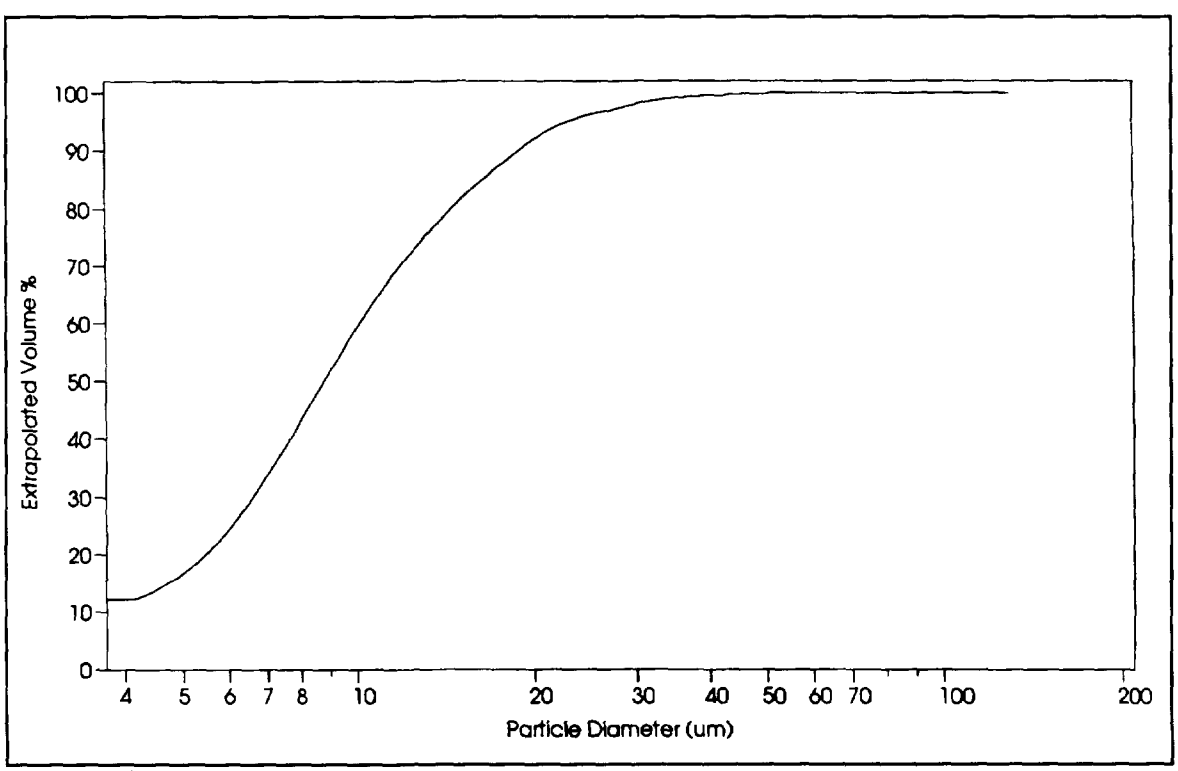

Figure A1-4. *The cumulative particle size distribution of the corrosion products obtained in test A4.*

APPENDIX 1

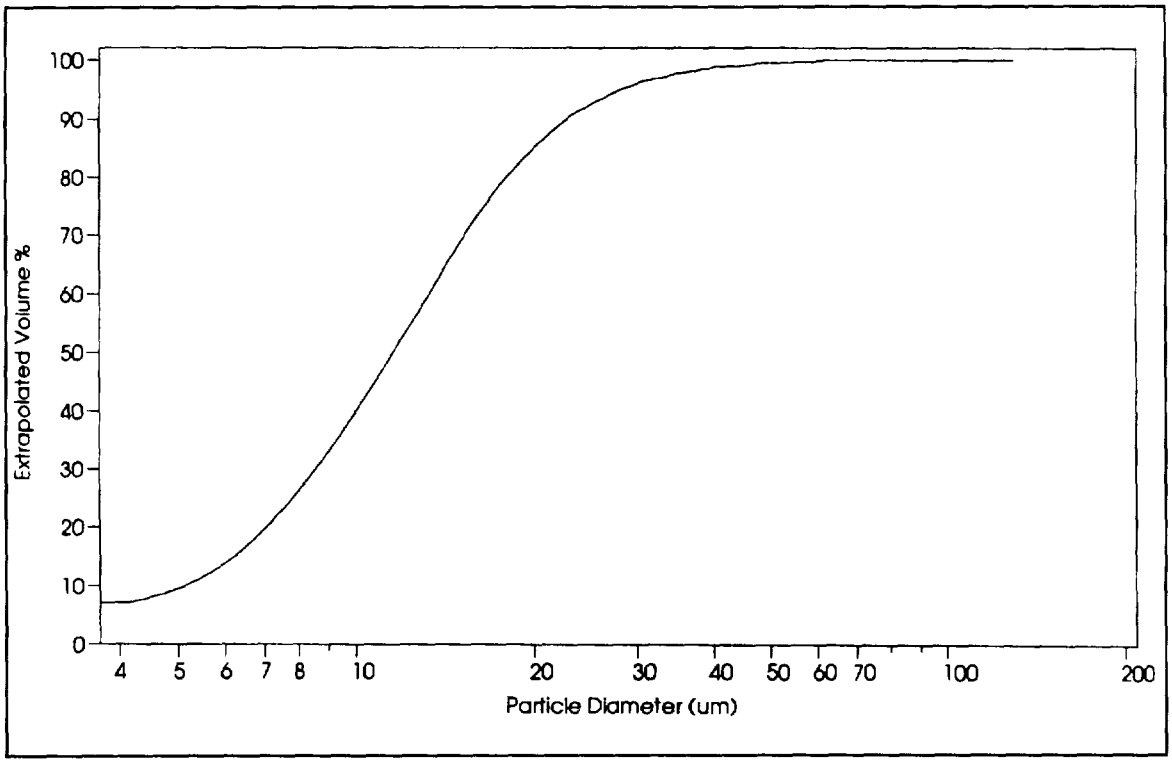

Figure A1-5. *The cumulative particle size distribution of the corrosion products obtained in test A5.*

APPENDIX 2

a) Corrosion rates (g/m²h) and wire radius decrease rates (μm/h) measured for zinc in a large pipe break case at different temperatures in different aqueous environments determined by measuring the resistance increase of the corroding wires.

t / °C	Weight loss rate of zinc / –dm/dt [g/(m²h)]				
	pH 8		pH 10		borate
	N_2	air	N_2	air	air
130	0.317	4.957	0.296	0.369	1.26
110	0.853	1.557	0.131	0.382	4.45
90	0.088	0.163	0.023	0.058	0.04
70	0.147	0.252	0.009	0.019	0.03
50	0.117	0.747	0.011	0.017	0.05
t / °C	**Wire radius decrease rate of zinc / –dr/dt [μm/h]**				
	pH 8		pH 10		borate
	N_2	air	N_2	air	air
130	0.0444	0.6943	0.0415	0.0517	0.1761
110	0.1195	0.2209	0.0184	0.0535	0.6231
90	0.0124	0.0229	0.0032	0.0081	0.0056
70	0.0206	0.0353	0.0012	0.0027	0.0042
50	0.0164	0.1047	0.0015	0.0024	0.007

b) Corrosion rates (g/m²h) and wire radius decrease rates (μm/h)measured for aluminium in a large pipe break case at different temperatures in different aqueous environments determined by measuring the resistance increase of the corroding wires.

t / °C	Weight loss rate of zinc / –dm/dt [g/(m²h)]				
	pH 8		pH 10		borate
	N_2	air	N_2	air	air
130	0.412	0.197	0.701	0.072	3.06
110	0.207	0.899	0.283	0.150	1.23
90	0.116	0.048	0.031	0.012	1.45
70	0.087	0.037	0.043	0.006	0.60
50	0.080	0.004	0.012	0.006	0.15
t / °C	**Wire radius decrease rate of zinc / –dr/dt [μm/h]**				
	pH 8		pH 10		borate
	N_2	air	N_2	air	air
130	0.1524	0.0731	0.2598	0.0267	1.1335
110	0.0767	0.3328	0.1049	0.0555	0.4539
90	0.0429	0.0178	0.0114	0.0046	0.537
70	0.0321	0.0137	0.0158	0.0022	0.222
50	0.0298	0.0014	0.0045	0.0022	0.0556

APPENDIX 3

Corrosion rates (g/m^2h) measured for zinc and aluminium in a severe accident case at 50 °C in aqueous environments (different pH and Cl^- concentrations) determined by measuring the resistance increase of the corroding wires.

pH	[HCl] / mol/l	[LiOH] / mol/l	Zn / –dm/dt / g/m^2h	Al / –dm/dt / g/m^2h
3	$1.0 \cdot 10^{-3}$	—	0.142	0.030
5	$1.0 \cdot 10^{-5}$	—	0.108	0.030
7	—	—	0.079	0.016
9	$5.0 \cdot 10^{-4}$	$5.6 \cdot 10^{-4}$	0.120	0.051
11	$5.0 \cdot 10^{-4}$	$7.0 \cdot 10^{-3}$	0.110	0.126